

Induced Transverse Spin Components in Longitudinally Polarized Beam at STAR

David Underwood
High Energy Physics
Argonne National Laboratory
Jan. 24, 2005

ROUGH DRAFT

Abstract

When protons pass through quadrupoles, there are large spin rotations. For example, ignoring the DX magnets, a beam with pure longitudinal polarization between the spin rotators and the low beta quadrupoles would have transverse components of spin at STAR. We have done a Monte-Carlo study of these effects. In most calculations we can ignore the small non-commutative effects of the actual spin directions from the RHIC Rotators and the DX magnets. However we have done one set of calculations with these effects, which give phi components of polarization. There are geometric effects which cause the two spin ANN not to cancel at locations away from $z=0$ vertex. There are both ANN and AN effects which will have a spatial distribution, which may be coupled to geometrical acceptance and steeply falling cross sections. Also, the AN effects may be enhanced by beam mis-steering or scraping.

Introduction

This study was motivated in two ways. Long ago, I did a study which showed that the spin precession at the edge of the beam in the combined final focusing for an SSC interaction region was 90 degrees. The spin in an individual quadrupole would be much larger, by at roughly an order of magnitude. More recently, People analyzing the spin data in STAR observed a dependence in the spin normalization which depended on vertex position along the beamline. In particular, within the large error bars, the deviations had the same sign on both sides of $z=0$ of the interaction region. It is important to note that these normalizations are established by detectors in STAR, and would be sensitive to real differences in the spin-spin cross sections.

A simplified example of the rotation in the STAR focusing is shown in figures 1 and 2. Basically, the further a particle is from the center of a quadrupole, (or doublet or triplet) the more the trajectory is bent in order to focus it at the interaction region. The "spin rotation" (in a classical picture) happens just as in a dipole bending the path, or in a snake magnet. A simple calculation gives a rotation of around 18 degrees at the edge of the 4.4 cm quad aperture at 100 GeV/c, assuming the center of the low beta quads is 27 meters from the focus. For longitudinal beam between the spin rotators and the low beta quads, this would give a maximum of 30 % transverse component at the edge of the beam,

and no transverse component in the middle. The actual beam size is considerably smaller than the quadrupole aperture.

A remarkable feature of the induced TRANSVERSE spin distributions in the STAR interaction region is that the product $P_{\text{blue}} \cdot P_{\text{yellow}}$ cancels at $z=0$ due to the overlap of all spin directions at the focus, but does not cancel away from $z=0$.

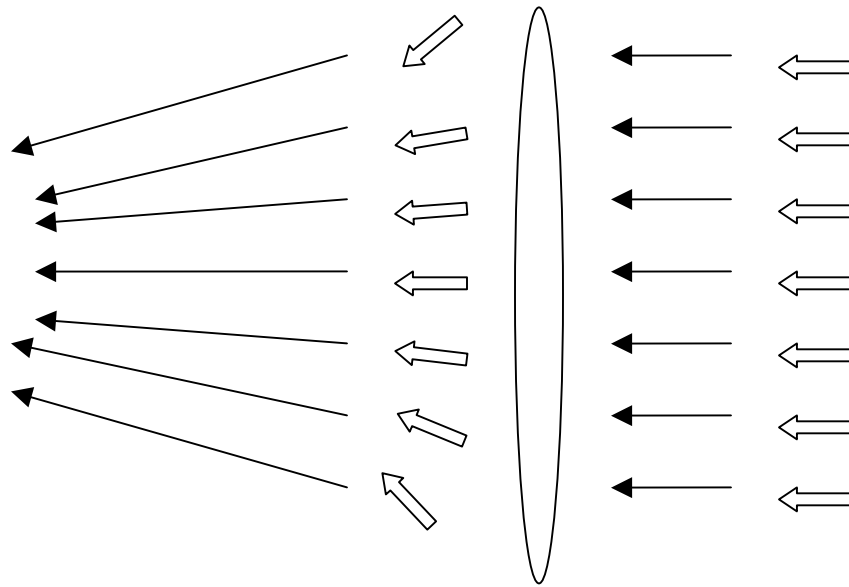


Figure 1) Parallel beam trajectories, and longitudinal polarization are transformed in a focusing element.

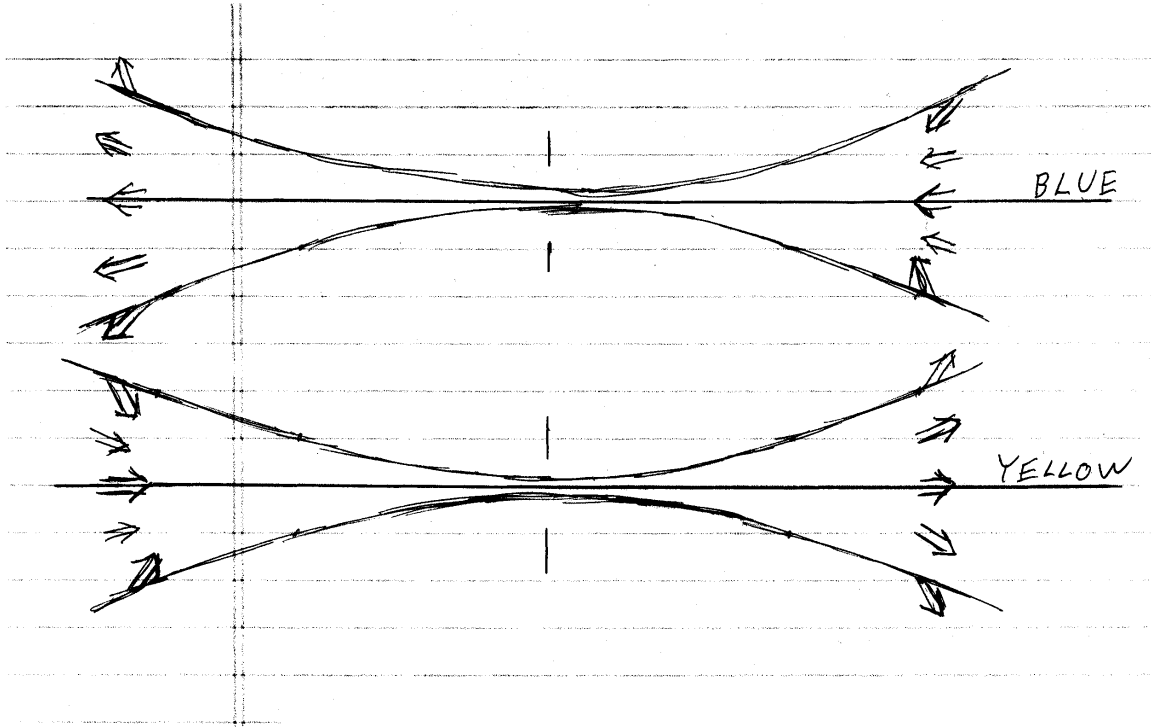


Figure 2) Spin directions at various locations in the colliding beam region.

In reality, the spin direction is not longitudinal at the entrance to the quadrupoles, but is rotated some 40 degrees about the vertical axis to be compensated by the rotations in the DX magnets. This modifies our simple assumptions only slightly. We can calculate the magnitude with the following ansatz: Start with longitudinal polarization. Rotate by 40 degrees about the vertical counter clock wise. Then rotate about the horizontal axis, magnitude depending on the size of the beam in the quadrupole. Then rotate back 40 degrees clockwise. For a 20 degree rotation about the horizontal axis in the quadrupole, (which would be a few sigma out on a typical beam) the net effect is a 2% reduction in longitudinal polarization, and a reduction of the effects in most of this paper by about 25% on one axis. For one calculation, we modified the MC program to actually do all the spin components and rotations beginning with polarization 40 degrees from longitudinal out of the RHIC rotators.

For this MC study, we have treated some parameters in a realistic way, eg, used measured beam bunch length distributions, and exaggerated other parameters, eg, beam diameter and mis-steering of beam in the quadrupole. The results in the case of the exaggerated parameters can be scaled, or further simulations can be done.

The beam was simulated in the transverse dimension with two different values, by using a gaussian distribution for the size at $z=0$ with $\sigma = 1$ mm and again with 100 microns. The beam angular distribution was simulated by using a gaussian size of $\sigma = 2$ cm at 27 meters from $z=0$, inside the low beta quads. Comparison with real beam parameters is made in the section on beam size and divergence.

The track and spin information for 10K beam tracks in blue, and the same number in yellow was generated and saved. Since we are interested in interactions of particles with various spin directions, a cross section was used to select realistic parts of the two beams interacting with each other. Cross sections were chosen to be quite small compared to beam dimensions. For the 1 mm beam sigma, we used a cross section of about 10^{-9} m², but this is quite small compared to beam dimensions.

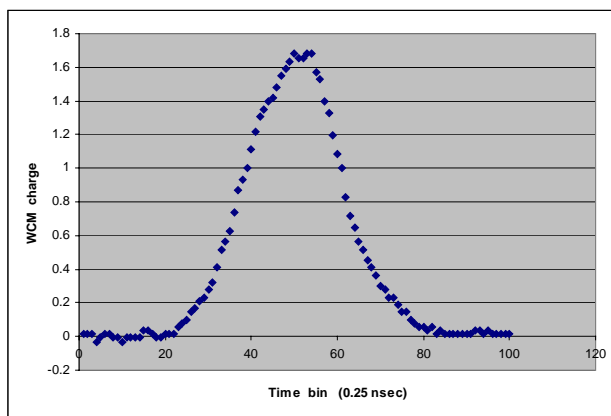


Figure 3) A normal beam bunch population measured with a beam current monitor for purposes of studying the RHIC polarimeter. The time bins are 0.25 ns, which is 7.5 cm. This normal bunch is about 60 bins, or 15 ns or 4.5 meters, base to base. Note

that the overlap of two bunches of this size gives a roughly gaussian vertex distribution with about 0.55 meter rms. (From H. Spinka, Bunch Studies, April, 2005)

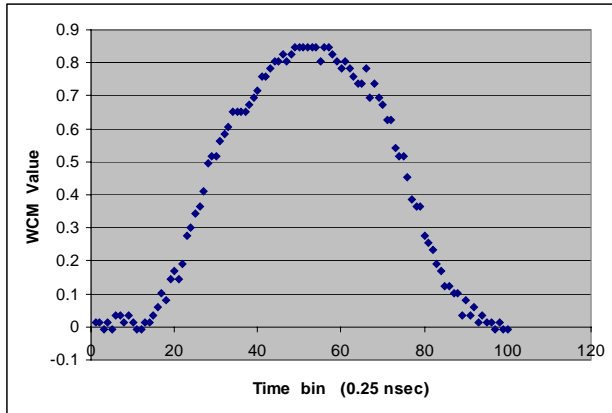


Figure 4) An example of a bad bunch within a bunch train. This one is about 90 time bins, or 22 ns or 6.6 meters long, base to base. (From H. Spinka, Bunch Studies, April, 2005)

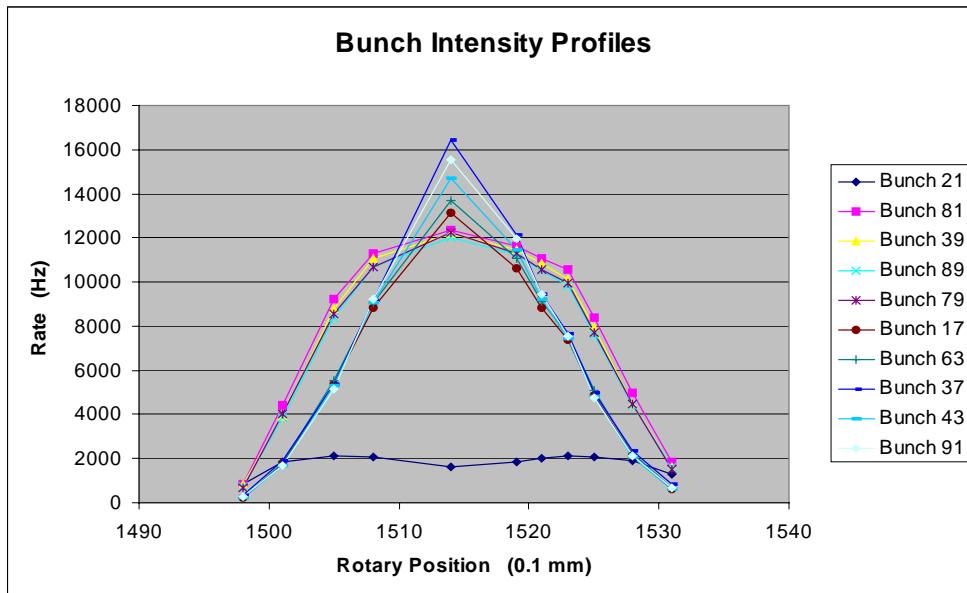


Figure 5) Examples of TRANSVERSE beam shape in a part of the machine far from STAR. Note that the shapes are not gaussian, but more like triangles. (From H. Spinka, Bunch Studies, April, 2005)

Local vs Global

The effects we treat in this paper are local within the accelerator lattice. To a good approximation, the rotations on one side of an interaction region are undone on the other side of the interaction region. Even the non-commutative rotations from orthogonal bends are canceled to the extent that beam trajectories are the mirror image on the two

sides of the interaction region. The extent to which this does not happen depends on a combination of emittance and beta function, so that not all trajectories cross the nominal beam axis at exactly $z=0$ in the interaction region, and thus are not at exactly the same radius within quadrupoles on either side of the interaction region. With perfect mechanical and magnetic symmetry, this would lead to intrinsic resonances depending on betatron oscillations. There can also be imperfection resonances, for example depending on magnet placement, inexact matching of rotator functions, etc.

Generally, the residual effects from this small non-cancellation at the local level are made to have negligible global effect by means of many turns in the accelerator, and by using the spin precession snakes to cancel small resonances.

There are other effects which are global in nature, and can produce unwanted spin components. For example, a transverse component of spin was observed in the CNI polarimeters in run 3 (?). This could arise from a mis-tuning of the snakes or rotators. This mis-tuning could be the result of the current settings, or mechanical variations among magnets.

As an example of a large global effect, it was proposed at one point to run with only one snake. In this case the stable spin direction would be in the horizontal plane in the accelerator, but would precess with position around the ring.

A Digression on Beam Size and Angles

Based on formulas in "The RHIC Accelerator" M. Harrison, S. Peggs, T. Roser
Ann. Rev Nucl Part Sci 2002. 52:425-69

Also based on measurements of RHIC beam in PHENIX, A. Drees, Private communication.

We use the formula for sigma of a beam:

$\sigma = \sqrt{(\epsilon * \beta \text{ function}) / 6\pi * (\gamma * \beta \text{ relativistic})}$
and ignore dispersion

where $(\gamma * \beta \text{ relativistic})$ is about 106 for 100 GeV/c protons,
 β function is roughly 1000 meters at low eta quads and roughly 1 meter at collision,
 ϵ is area of $dx.d\theta$ ellipse normalized to $(\gamma * \beta \text{ relativistic})$ and for 95% of beam particles. More about β at quads later.

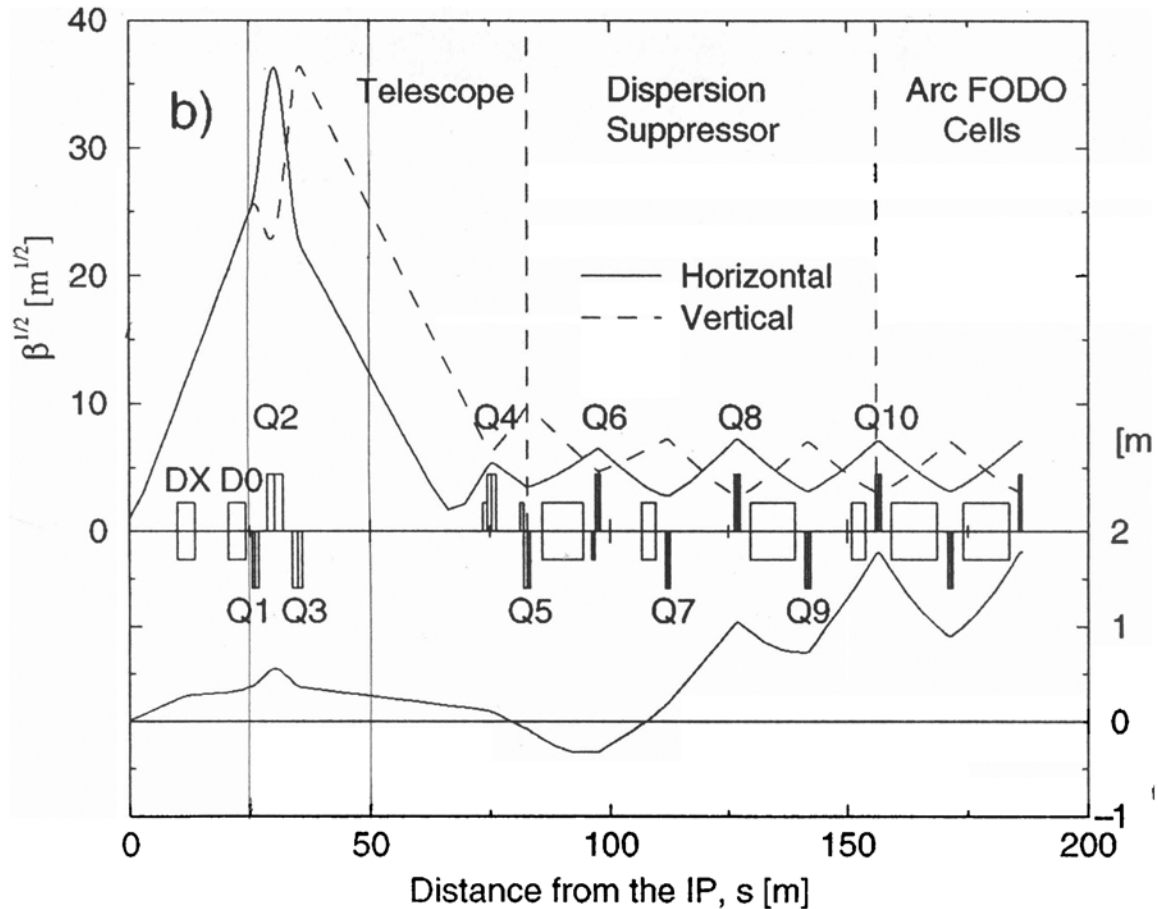
We assume round beams, with $\epsilon_x = \epsilon_y$.

Measured beam spot sizes in PHENIX range from 170 microns to 440 microns, with 230 micron typical.

These give ϵ from 18 μm^2 to 121 μm^2 . with typical 34 μm^2 , assuming $\beta^* = 1 \text{ m}$.

The β function we really want is the roughly linear part of $\sqrt{\beta}$ between the interaction vertex and the quadrupoles, not the much larger value inside Q2.

Reading off the picture from "The RHIC Accelerator" we see the root-beta is 25 at 25 M and extrapolates to 27 at 27 m. This gives $\beta = 730$ at 27 m. So, for what I have already run in the MC, assuming $\beta = 730$, sigma of beam is 2 cm at 27 meters. We get $\epsilon = 348 \text{ e-6}$, or 110 pi , which is large, but within what has been seen. However, this is 3 times typical, and beam size goes as $\sqrt{\epsilon}$ so the MC effects would only be 1.7 times typical if everything were gaussian.



Results

The MC beam size and divergence were plotted for illustration in PAW plots 101,102,103,104, (not shown) and the rms envelope in plots 201-230,(not shown) and summarized in figure 351 (see below) The beam crossing is shown in figures 495, 496, 501, with 495 showing the overlap product at one instant in time, and fig 496 showing the integral over the crossing, and the 2-D plot 501 showing the crossing product (luminosity vs z) as a function of time.

Next we show the spin components coming out of the low beta quads in figures 111,112,113,114, ignoring the phi components arising from non-commutative rotations.

Figures 156-158 with 151-153 demonstrate an effect which motivated this whole study. In figures 151 one can see that the radial spin components largely cancel at $z = 0$ where the correlation of slope with position goes to 0. The maximum residual is around $\pm 1/2$ percent radial polarization. As one moves away from $z=0$, the geometric effects become apparent, and one can see the magnitude of the radial component of polarization is zero in the center of the beam, but grows near the envelope. We use the quantity Polarization vector dot radius vs radius to show this. As we go further from $z=0$, the geometrical correlation of radial polarization vs radius becomes even stronger, as shown in figure 158. Figures 151-153 give an indication of the beam intensity associated with each radial position. These are plotted as integrals at each r , effectively $r \cdot I(r)$ vs r .

Figures 113 and 114 show the reduction in the longitudinal polarization which occurs due to rotation into the radial direction. For the case studied, with 2 cm rms beam in the low beta quads, this is several percent.

Two Figures are used to illustrate the MC methods, and two intermediate results. The first set (a) is for beam $\sigma = 1$ mm at the interaction point, and the second set (b) is for beam $\sigma = 0.1$ mm at the interaction point.

Fig 182 a and b) The separation between Blue and Yellow particles when they are within the interaction cross section. (cross section, radius= 2×10^{-4} m).

Fig 184 a and b) The Y(upward) component of polarization in the Blue beam exiting the low beta quadrupoles after severe scraping of the bottom half of the beam.

Fig 351 a and b) The beam σ vs z within ± 2.75 m of the interaction point.

Fig 364 a and b) The Luminosity times Pol (Trans., Yel.) times Pol (Trans., Blue) Vs z , with real bunch length, (Luminosity in arbitrary units).

Fig 366 a and b show the polarization weighted ratio (in %) of transverse 2-spin luminosity to longitudinal 2-spin luminosity, vs z of the vertex. Integrated over beam radius.

Fig 367 a and b show the polarization weighted ratio (in %) of transverse (radial) polarization in Blue interacting with anything in Yellow, relative to the probability of longitudinal interacting on longitudinal. (creates AN locally)

We next look at the Luminosity relevant to ATT. Figure 368 shows that for a round, symmetrical beam, and for the realistic bunch lengths limiting the distance from $z=0$, the integrated Luminosity times (P blue tran dot P yellow tran) is less than 2% of the longitudinal 2-spin Luminosity, and it goes to zero at $z=0$. It does have the same sign on both sides of $z=0$, as guessed initially. Also, this plot is the integral over beam radius, and the effects are a strong function of radius as suggested by figure 158.

Fig 368 a and b show the polarization weighted ratio (in %) of upward polarization interacting with anything, relative to longitudinal on longitudinal. The downward component of polarization in the Blue beam has been eliminated by scraping, which is equivalent to beam mis-steering in the low-beta quadrupoles. This is large.

Fig 369 a and b show the polarization weighted ratio (in %) of horizontal polarization interacting with anything, relative to longitudinal on longitudinal. This is small because

the amount of left polarization on one side of the beam is equal to the amount of right polarization on the other side of the beam.

Summary

We have simulated some transverse spin effects for a nominal situation of two longitudinally polarized colliding beams. Our assumptions about the nature of the beams enhance the effects we found somewhat over what is typical, but not beyond situations which have actually happened.

There are large transverse, radial, spin components in the beam, which are spatially separated from the more pure longitudinal parts of the beam. The effects tend to cancel because of the symmetry of the beam and the finite length of the beam bunch.

The integrated luminosity for ATT relative to ALL is fairly small, from zero in the middle to 2% at the ends of the interaction diamond, with a z distribution which depends on the emittance. However, the effect could still be over 15% at some locations of the vertex near the outside of the beam. We don't know whether or not some physics analyses could be more sensitive to this part of the interaction diamond.

The luminosity for the single spin asymmetry, AN, relative to the nominal two-spin longitudinal, ALL, can be quite large, 10% of all interactions, if the beam is either mis-steered or scraped.

We are largely concerned with the spin luminosity normalizations as measured by the beam-beam counters. With beam polarizations of 50% each, there is another factor of 2 in single-spin polarization times luminosity over what would be observed from two-spin LL in beam-beam counters. We don't know the physics spin asymmetries at low pt at the eta range of the BBC counters. So far at higher PT and higher eta the single spin physics asymmetries are larger than what we have seen in the central region in two spin asymmetries.

For BBC counter acceptance which is azimuthally or mirror symmetric, it is hard to get substantial effects in the BBC counters from these induced spin components, even when they are large, such as 10%.

- a) If physics Att and All are anywhere near the same magnitude at the low pt going into the BBC, the 1 to 2 % luminosity $*P1 *P2$ for Att will not be a big effect.
- b) For radial single spin, which is large, the effects are cancelled by the symmetry in the beam around the nominal axis, and again by the symmetry of the detectors around the nominal axis (assuming these symmetries exist).
- c) For one-direction single spin due to beam scraping or mis-alignment, the effects in the BBC counters cancel by symmetry of the counters. I don't think there are dead channels or deliberate cuts which destroy this. Do errors in the timing cuts affect this?

As an example, to get 0.3 % asymmetry in the BBC, we might have 5% transverse spin component, 15 % difference in the left vs right efficiency of the BBC counters, and 40% transverse spin physics asymmetry.

d) For phi components of spin, the effect at a given BBC counter from the difference in pt from the two sides of the beam (with slightly different angles due to divergence) seems small, assuming some simple cross section at low pt, like $\exp(-6*pt)$.

References

“Bunch Studies”, H. Spinka, Brookhaven C-A/AP/206, May 13, 2005.

"The RHIC Accelerator" M. Harrison, S. Peggs, T. Roser
Ann. Rev Nucl Part Sci 2002. 52:425-69

Measurements of RHIC beam in PHENIX, A. Drees, Private communication.

List of PAW histograms from the two MC programs.

(The two are beam round and beam scrapped off at the bottom)
Most are alike for beam round vs scrapped, but ones with upward polarization interacting on anything in other beam are quite different with beam scraping (hists 357, 359, 368, 369)

101 x vtx blue
102 y vtx blue
103 slope x blue
104 slope y blue

111 spin x component blue
112 spin y component blue
113 spin z component blue .96 to 1
114 spin z component blue .9 to 1

151 $r \cdot I(r)$ vs r at z=0
152 $r \cdot I(r)$ vs r at z=.6m
153 $r \cdot I(r)$ vs r at z=1.05m
156 P dot r vs r at z = 0
157 P dot r vs r at z=.6m
158 P dot r vs r at z = 1.05m

181 track separation at some Z
182 track separation within cross section
183 spin x blue for interacting tracks
184 spin y blue for interacting tracks

201 to 230 beam rms vs z (226 is at z=0)

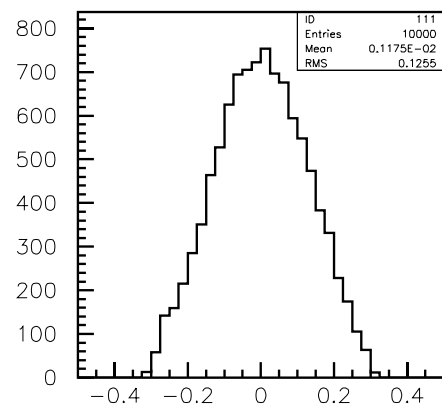
351 sigma beam vs z
352 Luminosity variation due to divergence
353 Lum .P1t.P2t vs z, (inf. bunch len)
354 Lum .P1L.P2L vs z, (inf bunch len)
355 P blue tran dot Pyt vs z (inf bunch len)
356 P blue tran on anything vs z (inf bunch len)
357 P blue upward on anything (bottom half beam cut) (inf bunch len)
358 debuggiung sum
359 P blue sideways on anything (bottom half beam cut)(inf bun len)

361 Lum vs z, inf bunch length
362 Lum vs z, real bunch length

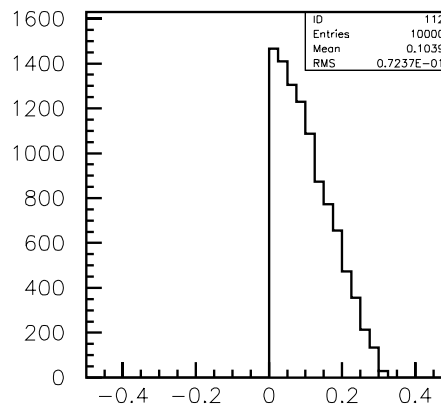
363 duplicate
364 Lum of P blu tran on P yel tran vs z (real bunch length)
365 ratio (Lum tran.tran)/ (Lum long.long) vs z (inf bunch len)
366 ratio (Lum tran.tran)/ (Lum long.long) vs z (real bunch len)
367 ratio (Lum tran.anything)/(Lum long.long) vs z (bottom cut)
368 ratio (Lum pol up on any)/(Lum long.long) vs z (bottom beam cut)
369 ratio (Lum pol sideways on any)/(Lum long.long) vs z (bottom cut)

495 beam-beam overlap with bunches centered
496 integral of beam-beam overlap over a full crossing

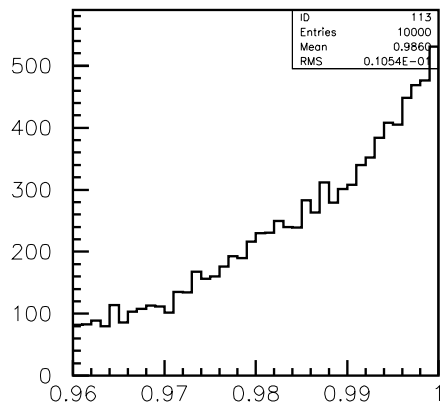
501 2-d plot of bunch-bunch product over time



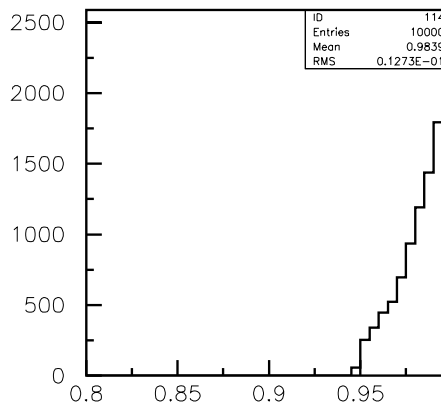
spinx blue



spiny blue



spinz blue

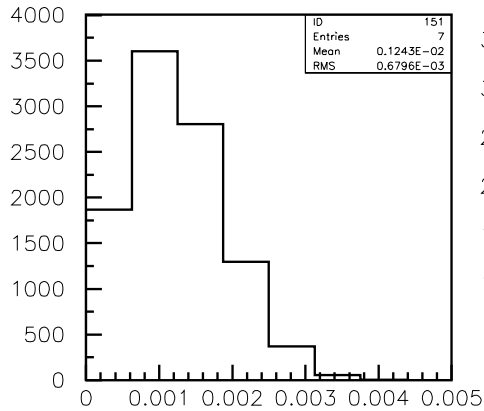


spinz blue

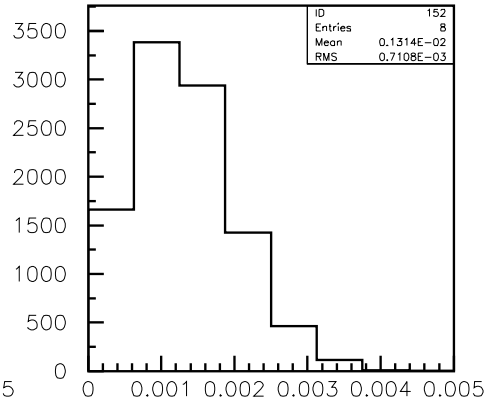
Fig 111 The spin component in the horizontal direction near the low beta quads, integrated over beam radius.

Fig 112 The vertical spin component near the low beta quads, integrated over beam radius. The negative polarization is missing because the bottom half of the beam has been removed. This scraping is roughly equivalent to mis-steering the beam in the quadrupoles.

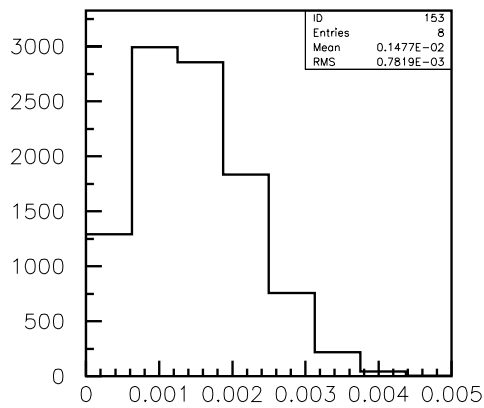
Fig 113 and 114 The z component of spin remaining in the beam after the low beta quadrupoles.



R*(l) vs r, z=0



R*(l) vs r, z=.6

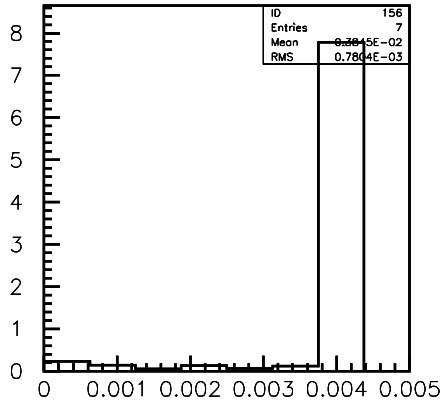


R*(l) vs r, z=1.05

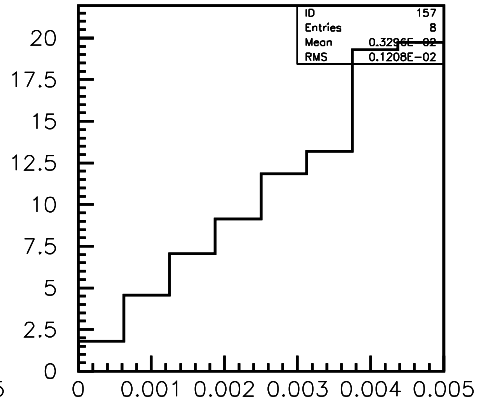
Fig 151 The beam intensity (r times $I(r)$) vs radius at $z=0$. This is shown in the same bins as the transverse polarization vs radius (Fig 156) to aid in understanding the significance of the spin components.

Fig 152 The beam intensity (r times $I(r)$) vs radius at $z=0.6$ meter. This is shown in the same bins as the transverse polarization vs radius (Fig 157) to aid in understanding the significance of the spin components.

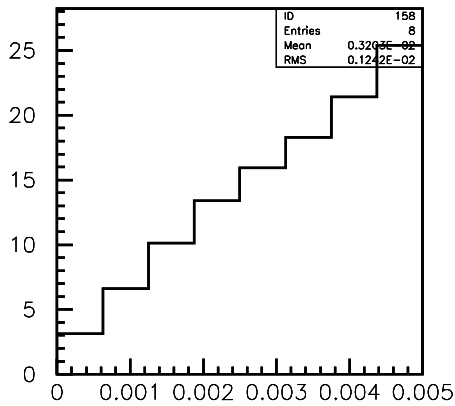
Fig 153 The beam intensity (r times $I(r)$) vs radius at $z=1.05$ meter. This is shown in the same bins as the transverse polarization vs radius (Fig 158) to aid in understanding the significance of the spin components.



Pdotr vs r,z, z=0



Pdotr vs r,z, z=.6

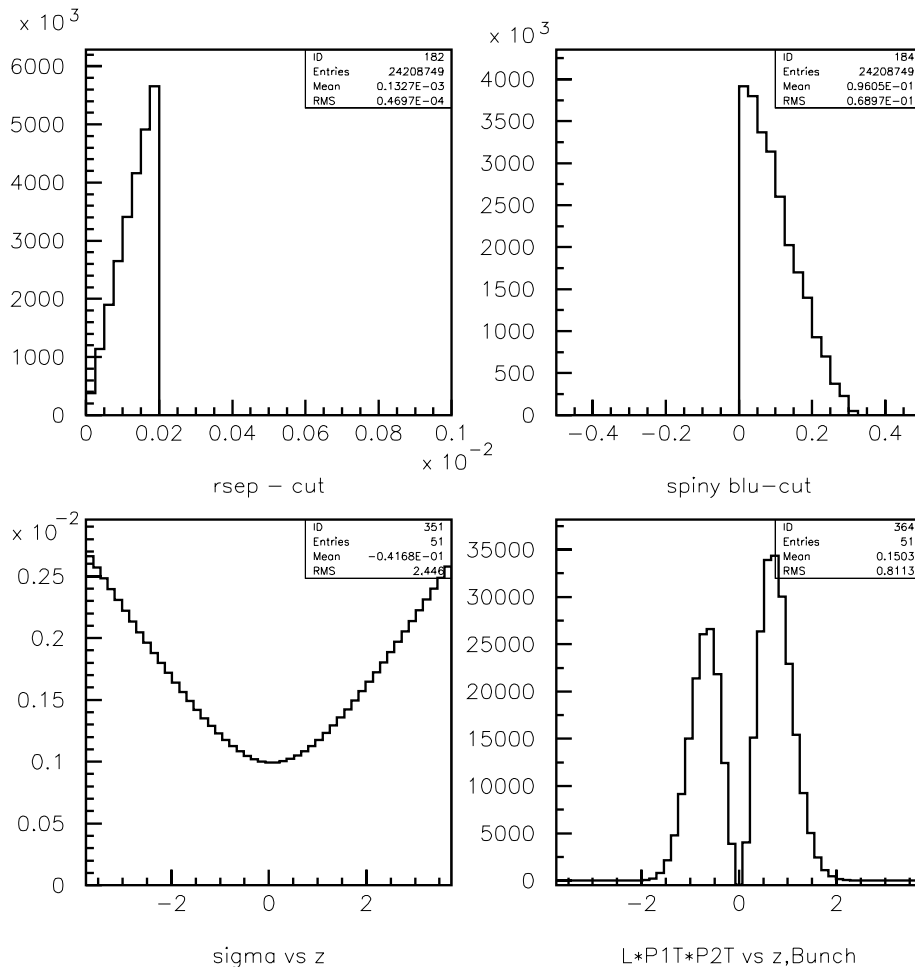


Pdotr vs r,z, z=1.05

Fig 156 The transverse polarization (in %) in the beam at $z=0$. The large value at .004 meters is a fluctuation where there is almost no intensity, many sigma from the center of the beam.

Fig 157 The transverse polarization (in %) as a function of radius in the beam at $z=0.6$ meter.

Fig 158 The transverse polarization (in %) as a function of radius in the beam at $z=1.05$ meter.



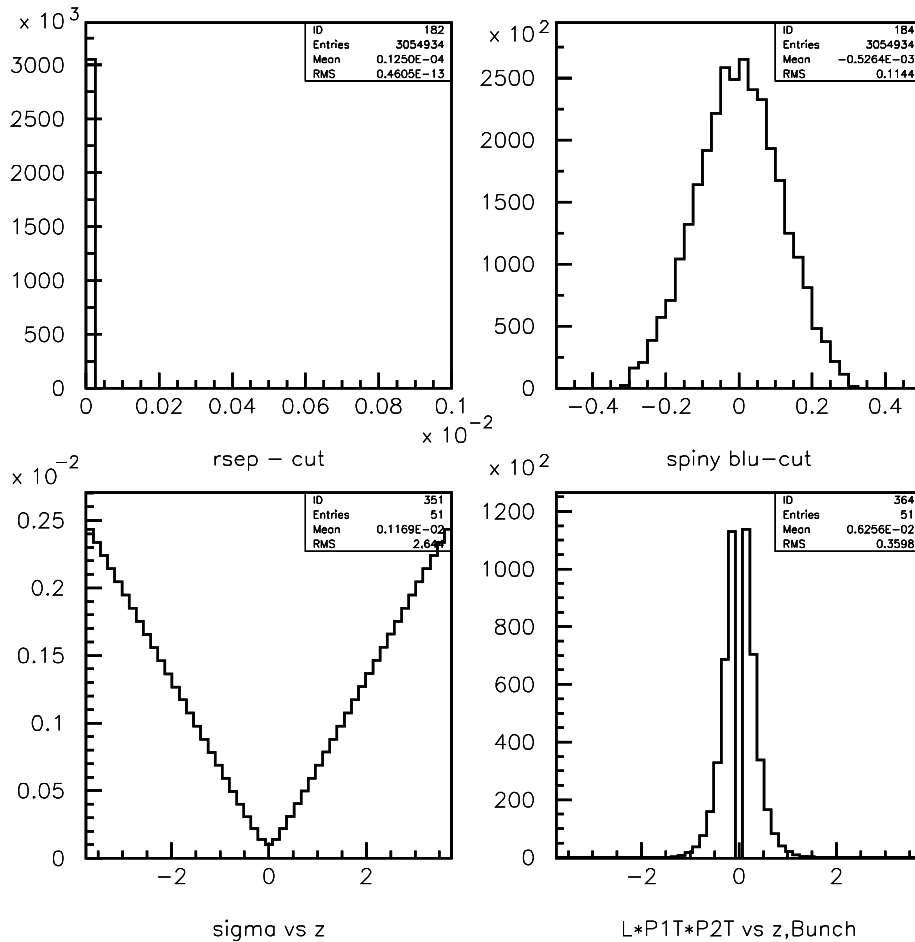
Two Figures used to illustrate the MC methods, and two intermediate results. This set (a) is for beam sigma = 1 mm at the interaction point.

Fig 182 a) The separation between Blue and Yellow particles when they are within the interaction cross section. (cross section, radius= 2×10^{-4} m).

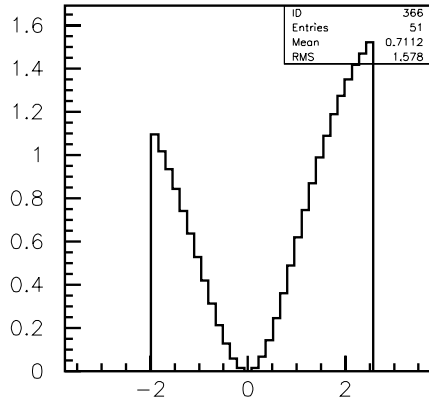
Fig 184 a) The Y(upward) component of polarization in the Blue beam exiting the low beta quadrupoles after severe scraping of the bottom half of the beam.

Fig 351 a) The beam sigma vs z within +/- 2.75 m of the interaction point.

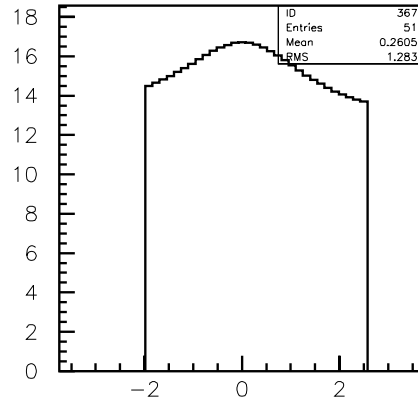
Fig 364 a) The Luminosity times Pol (Trans., Yel.) times Pol (Trans., Blue) Vs z , with real bunch length, (Luminosity in arbitrary units).



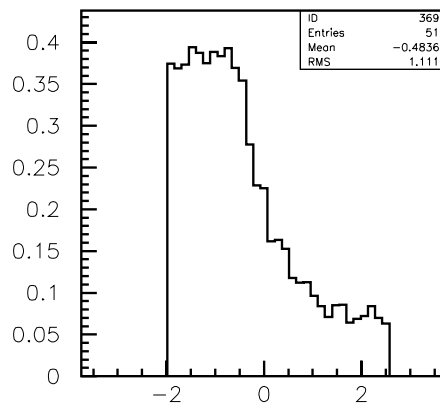
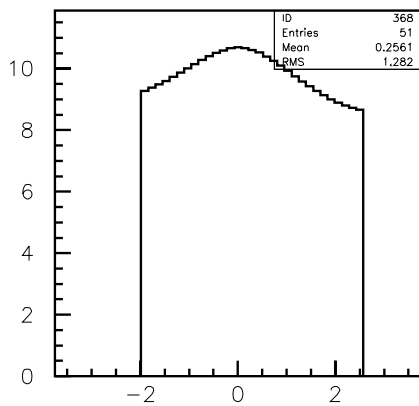
This set (a) is for beam $\sigma = 0.1$ mm at the interaction point.
 Two Figures used to illustrate the MC methods, and two intermediate results.
 Fig 182 b) The separation between Blue and Yellow particles when they are within the interaction cross section. (cross section, radius= 5×10^{-5} m).
 Fig 184 b) The Y(upward) component of polarization in the Blue beam exiting the low beta quadrupoles after severe scraping of the bottom half of the beam.
 Fig 351 b) The beam σ vs z within ± 2.75 m of the interaction point.
 Fig 364 b) The Luminosity times Pol (Trans., Yel.) times Pol (Trans., Blue) Vs z , with real bunch length, (Luminosity in arbitrary units).



trans P1P2/long P1P2 real bunch len z



trans P1.any/long P1P2 real bunch len z



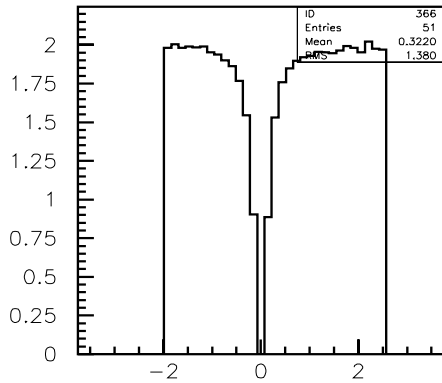
This set (a) for sigma beam = 1 mm at interaction point.

Fig 366 a) The polarization weighted ratio (in %) of transverse 2-spin luminosity to longitudinal 2-spin luminosity, vs z of the vertex. Integrated over beam radius.

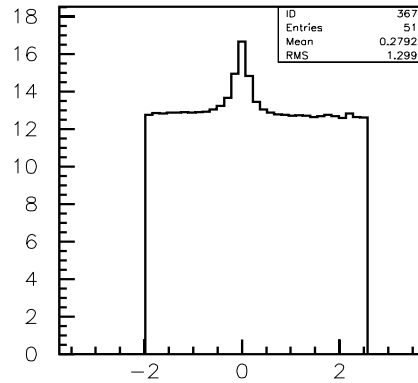
Fig 367 a) The polarization weighted ratio (in %) of transverse (radial) polarization in Blue interacting with anything in Yellow, relative to the probability of longitudinal interacting on longitudinal. (creates AN locally)

Fig 368 a) The polarization weighted ratio (in %) of upward polarization interacting with anything, relative to longitudinal on longitudinal. The downward component of polarization in the Blue beam has been eliminated by scraping, which is equivalent to beam mis-steering in the low-beta quadrupoles. This is large.

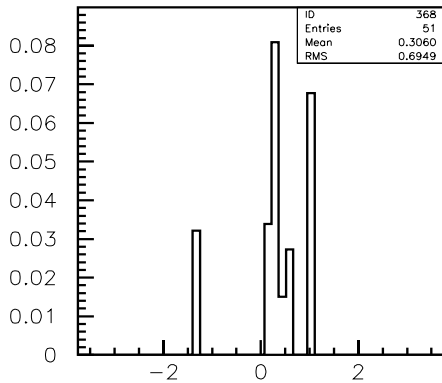
Fig 369 a) The polarization weighted ratio (in %) of horizontal polarization interacting with anything, relative to longitudinal on longitudinal. This is small because the amount of left polarization on one side of the beam is equal to the amount of right polarization on



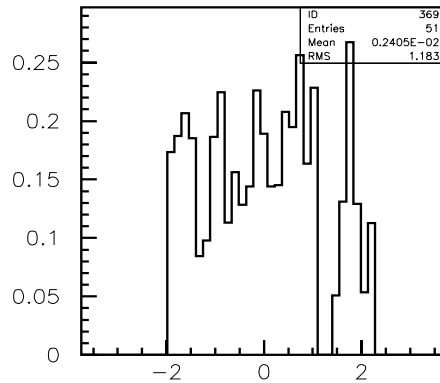
trans P1P2/long P1P2 real bunch len z



trans P1.any/long P1P2 real bunch len z



P1-up.any/long P1P2 real bunch len z



P1-side.any/long P1P2 real bunch len z

This set (b) for sigma beam =0.1 mm at the interaction point.

Fig 366 b)The polarization weighted ratio (in %) of transverse 2-spin luminosity to longitudinal 2-spin luminosity, vs z of the vertex. Integrated over beam radius.

Fig 367 b) The polarization weighted ratio (in %) of transverse (radial) polarization in Blue interacting with anything in Yellow, relative to the probability of longitudinal interacting on longitudinal. (creates AN locally)

Fig 368 b)The polarization weighted ratio (in %) of upward polarization interacting with anything, relative to longitudinal on longitudinal. The downward component of polarization in the Blue beam has been eliminated by scraping, which is equivalent to beam mis-steering in the low-beta quadrupoles. This is large.

Fig 369 b) The polarization weighted ratio (in %) of horizontal polarization interacting with anything, relative to longitudinal on longitudinal. This is small because the amount of left polarization on one side of the beam is equal to the amount of right polarization on

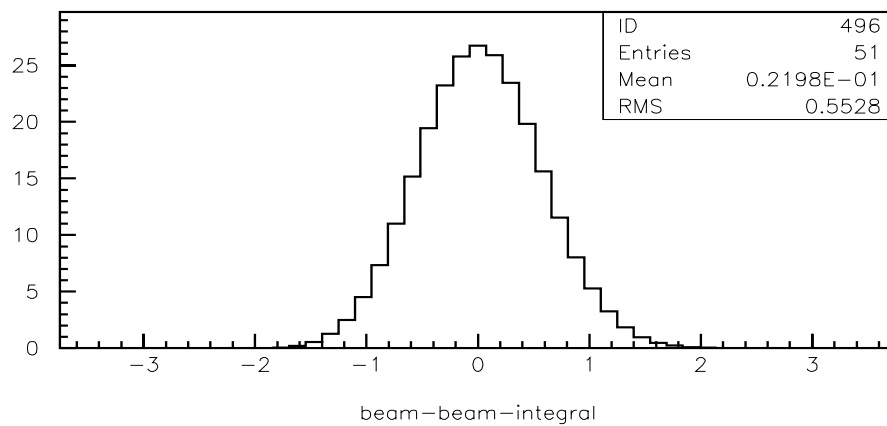
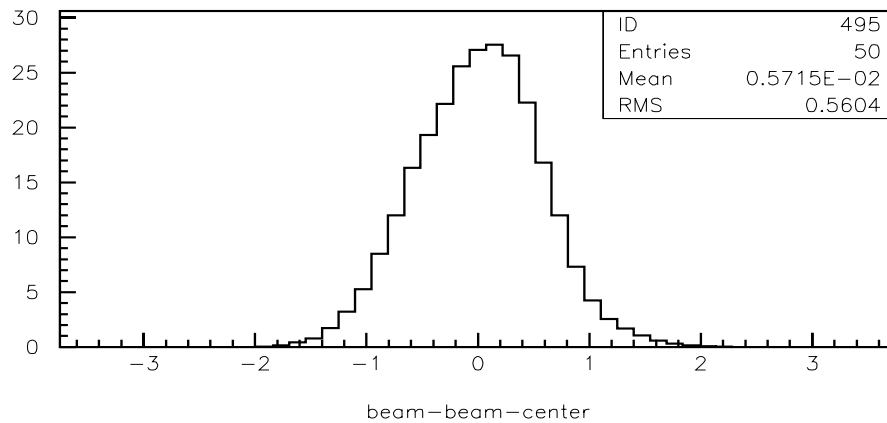


Fig 495 The instantaneous overlap of Blue and Yellow bunches when they are at $z=0$.

Fig 496 The integral of the bunch crossing over the entire time of the crossing.

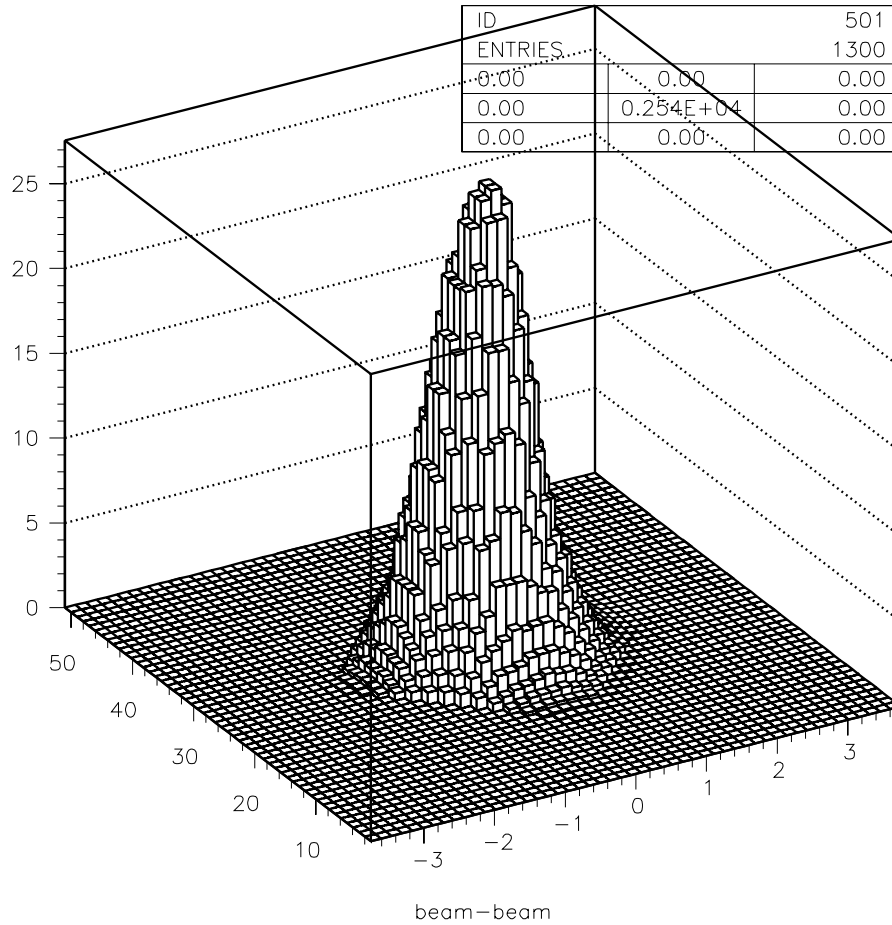


Fig 501 The longitudinal bunch crossing as a function of time. The range is from -3.75 meters to +3.75 meters and the time sequence is 51 steps of 0.5 ns (15 cm) .

